INVITED PAPER

Position Estimation via Ultra-Wide-Band Signals

UWB systems that first estimate time-of-arrival seem particularly well suited for precise estimation of their geolocation; noise, signal distortion, signal design and hardware design also influence achievable accuracy.

By Sinan Gezici, *Member IEEE* and H. Vincent Poor, *Fellow IEEE*

ABSTRACT | The high time resolution of ultra-wide-band (UWB) signals facilitates very precise position estimation in many scenarios, which makes a variety applications possible. This paper reviews the problem of position estimation in UWB systems, beginning with an overview of the basic structure of UWB signals and their positioning applications. This overview is followed by a discussion of various position estimation techniques, with an emphasis on time-based approaches, which are particularly suitable for UWB positioning systems. Practical issues arising in UWB signal design and hardware implementation are also discussed.

KEYWORDS | Impulse radio (IR); parameter estimation; ranging; time-of-arrival (TOA); ultra-wide-band (UWB)

I. ULTRA-WIDE-BAND SIGNALS AND POSITIONING APPLICATIONS

A. Ultra-Wide-Band Signals

Ultra-wide-band (UWB) signals are characterized by their very large bandwidths compared to those of conventional narrow-band/wide-band signals. According to the Federal Communications Commission (FCC), a UWB signal is defined to have an absolute bandwidth of at least 500 MHz or a fractional (relative) bandwidth of larger than 20% [1]. As shown in Fig. 1, the absolute bandwidth is obtained as the difference between the upper frequency f_H of the -10 dB emission point and the lower frequency f_L of the -10 dB emission point; i.e.,

$$B = f_H - f_L \tag{1}$$

which is also called -10 dB *bandwidth*. On the other hand, the fractional bandwidth is calculated as

$$B_{frac} = \frac{B}{f_c} \tag{2}$$

where f_c is the center frequency and is given by

$$f_c = \frac{f_H + f_L}{2}. \tag{3}$$

From (1) and (3), the fractional bandwidth B_{frac} in (2) can also be expressed as

$$B_{frac} = \frac{2(f_H - f_L)}{f_H + f_L}. \tag{4}$$

As UWB signals occupy a very large portion in the spectrum, they need to coexist with the incumbent systems without causing significant interference. Therefore, a set of regulations are imposed on systems transmitting UWB signals. According to the FCC regulations, UWB systems must transmit below certain power levels in order not to cause significant interference to the legacy systems in the same frequency spectrum. Specifically, the average power

Manuscript received September 28, 2007; revised May 13, 2008. First published February 27, 2009; current version published March 18, 2009. This work was supported in part by the European Commission under the framework of the FP7 Network of Excellence in Wireless COMmunications NEWCOM++ under Contract 216715 and in part by the National Science Foundation under Grants ANI-03-38807 and CNS-06-25637.

S. Gezici is with the Department of Electrical and Electronics Engineering, Bilkent University, Bilkent, Ankara TR-06800, Turkey (e-mail: gezici@ee.bilkent.edu.tr).
H. V. Poor is with the Department of Electrical Engineering, Princeton University, Princeton, NJ 08544 USA (e-mail: poor@princeton.edu).

Digital Object Identifier: 10.1109/JPROC.2008.2008840

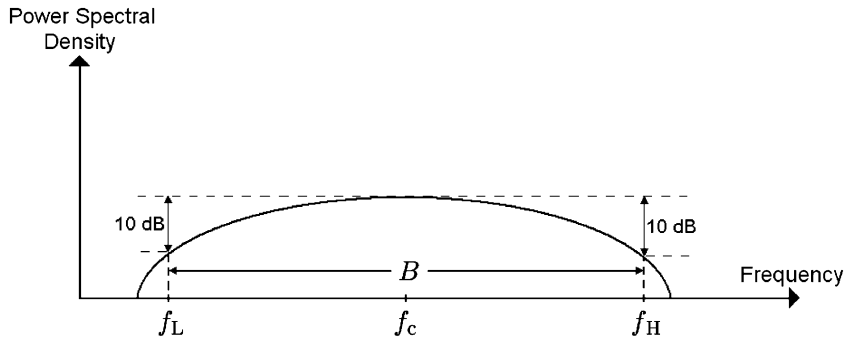

Fig. 1. *A UWB signal is defined to have an absolute bandwidth B of at least 500 MHz, or a fractional bandwidth B_{frac} larger than 0.2 [see (4)] [2].*

spectral density (PSD) must not exceed −41.3 dBm/MHz over the frequency band from 3.1 to 10.6 GHz, and it must be even lower outside this band, depending on the specific application [1]. For example, Fig. 2 illustrates the FCC limits for indoor communications systems. After the FCC legalized the use of UWB signals in the United States, a considerable amount of effort has been put into development and standardization of UWB systems [3], [4]. Both Japan and Europe recently allowed the use of UWB systems under certain regulations [5], [6].

Because of the inverse relation between the bandwidth and the duration of a signal, UWB systems are characterized by very short duration waveforms, usually on the order of a nanosecond. Commonly, a UWB system transmits very short duration pulses with a low duty cycle; that is, the ratio between the pulse transmission instant and the average time between two consecutive transmissions is usually kept small, as shown in Fig. 3. Such a pulse-based UWB signaling scheme is called *impulse radio* (IR) UWB [7]. In an IR UWB communications system, a number of UWB pulses are transmitted per information symbol, and information is usually conveyed by the timings or the polarities of the pulses.[1] For positioning systems, the main purpose is to estimate position related parameters of this IR UWB signal, such as its time-of-arrival (TOA), as will be discussed in Section II.

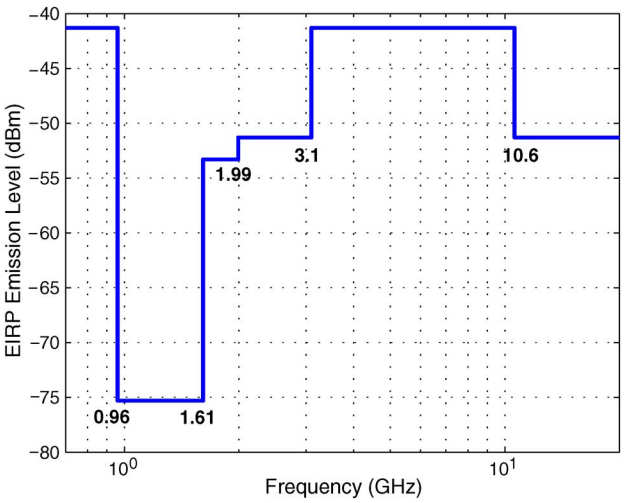

Fig. 2. *FCC emission limits for indoor UWB systems. Please refer to [1] for the regulations for imaging, vehicular radar, and outdoor communications systems. Note that the limits are specified in terms of equivalent isotropically-radiated power (EIRP), which is defined as the product of the power supplied to an antenna and its gain in a given direction relative to an isotropic antenna. According to the FCC regulations, emissions (EIRPs) are measured using a resolution bandwidth of 1 MHz.*

Large bandwidths of UWB signals bring many advantages for positioning, communications, and radar applications [2]:

- penetration through obstacles;
- accurate position estimation;
- high-speed data transmission;
- low cost and low power transceiver designs.

The penetration capability of a UWB signal is due to its large frequency spectrum that includes low-frequency components as well as high-frequency ones. This large spectrum also results in high time resolution, which improves ranging (i.e., distance estimation) accuracy, as will be discussed in Section II.

The appropriateness of UWB signals for high-speed data communications can be observed from the Shannon capacity formula. For an additive white Gaussian noise (AWGN) channel with bandwidth of B Hz, the maximum data rate that can be transmitted to a receiver with negligible error is given by

$$C = B\log_2(1+\mathrm{SNR}) \quad \text{(bits/s)} \tag{5}$$

[1]In addition to IR UWB systems, it is also possible to realize UWB systems with continuous transmissions. For example, direct-sequence code-division multiple-access systems with very short chip intervals can be classified as a UWB communications system [8]. Alternatively, transmission and reception of very short duration orthogonal frequency-division multiplexing (OFDM) symbols can be considered as an OFDM UWB scheme [9]. However, the focus of this paper will be on IR UWB systems.

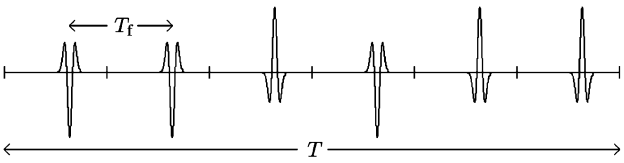

Fig. 3. *An example UWB signal consisting of short duration pulses with a low duty cycle, where T is the signal duration and T_f represents the pulse repetition interval or the frame interval.*

where SNR is the signal-to-noise ratio of the system. In other words, as the bandwidth of the system increases, more information can be sent from the transmitter to the receiver. Also note that for large bandwidths, signal power can be kept at low levels in order to increase the battery life of the system and to minimize the interference to the other systems in the same frequency spectrum.

Moreover, a UWB system can be realized in baseband (carrier-free), that is, UWB pulses can be transmitted without a sine-wave carrier. In that case, it becomes possible to design transmitters and receivers with fewer components [2].

B. UWB Positioning Applications

For positioning systems, UWB signals provide an accurate, low cost, and low power solution thanks to their unique properties discussed above. Especially, short-range wireless sensor networks (WSNs), which combine low/medium data-rate communications with positioning capability, seem to be the emerging application of UWB signals [10]. Some important applications of UWB WSNs can be exemplified as follows [2], [10], [11]:

- *Medical:* wireless body area networking for fitness and medical purposes, and monitoring the locations of wandering patients in a hospital;
- *Security/Military:* locating authorized people in high-security areas and tracking the positions of the military personnel;
- *Inventory Control:* real-time tracking of shipments and valuable items in manufacturing plants, and locating medical equipments in hospitals;
- *Search and Rescue:* locating lost children, injured sportsmen, emergency responders, miners, avalanche/earthquake victims, and firefighters;
- *Smart Homes:* home security, control of home appliances, and locating inhabitants.

Accuracy requirements of these positioning scenarios vary depending on the specific application [11]. For most applications, an accuracy of less than a foot is desirable, which makes UWB signaling a unique candidate in those scenarios.

The opportunities offered by UWB WSNs also resulted in the formation of the IEEE 802.15 low-rate alternative PHY task group (TG4a) in 2004 to design an alternate PHY specification for the already existing IEEE 802.15.4 standard for wireless personal-area networks [12]. The main aim of the TG4a was to provide communications and high-precision positioning with low power and low cost devices [13]. In March 2007, IEEE 802.15.4a was approved as a new amendment to IEEE Standard 802.15.4-2006. The 15.4a amendment specifies two optional signaling formats based on UWB and chirp spread spectrum (CSS) signaling [3]. The UWB option can use 250–750 MHz, 3.244–4.742 GHz, or 5.944–10.234 GHz bands, whereas the CSS uses the 2.4–2.4835 GHz band. Although the CSS option can only be used for communications purposes, the UWB option has an optional ranging capability, which facilitates new applications and market opportunities offered by UWB positioning systems.

UWB positioning systems have also attracted significant interest from the research community. Recent books on UWB systems and in general on wireless networks study UWB positioning applications as well [14]–[16]. In addition, research articles on UWB positioning, such as [10] and references therein, consider various aspects of position estimation based on UWB signals. The main purpose of this paper is to present a general overview of UWB positioning systems and present not only signal processing issues as in [10] but also practical design constraints, such as limitations on hardware components.

II. POSITION ESTIMATION TECHNIQUES

In order to comprehend the high-precision positioning capability of UWB signals, position estimation techniques should be investigated first. Position estimation of a node[2] in a wireless network involves signal exchanges between that node (called the 'target' node; i.e., the node to be located) and a number of reference nodes [17]. The position of a target node can be estimated by the target node itself, which is called *self-positioning*; or it can be estimated by a central unit that gathers position information from the reference nodes, which is called *remote-positioning* (*network-centric positioning*) [18]. In addition, depending on whether the position is estimated from the signals traveling between the nodes directly or not, two different position estimation schemes can be considered, as shown in Fig. 4 [2], [17]. *Direct positioning* refers to the case in which the position is estimated directly from the signals traveling between the nodes [19]. On the other hand, a *two-step positioning* system first extracts certain signal parameters from the signals and then estimates the position based on those signal parameters. Although the two-step positioning approach is suboptimal in general, it can have significantly lower complexity than the direct approach. Also, the performance of the two approaches is usually

[2]A "node" refers to any device involved in the position estimation process, such as a wireless sensor or a base station.

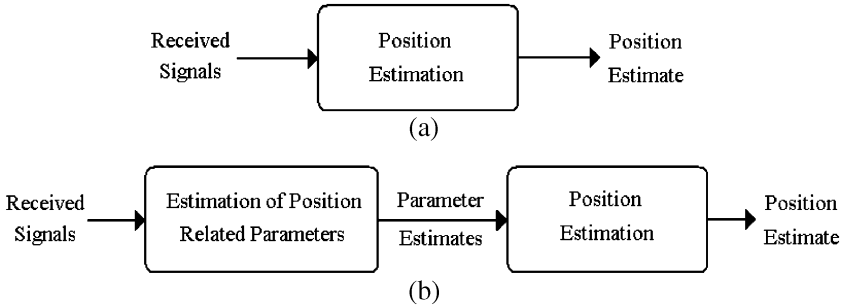

Fig. 4. *(a) Direct positioning and (b) two-step positioning [17].*

quite close for sufficiently high signal bandwidths and/or SNRs [19], [20]. Therefore, the two-step positioning is the common technique in most positioning systems, which will also be the main focus of this paper.

In the first step of a two-step positioning technique, signal parameters, such as TOA, angle-of-arrival (AOA), and/or received signal strength (RSS), are estimated. Then, in the second step, the target node position is estimated based on the signal parameters obtained from the first step [Fig. 4(b)]. In the following, various techniques for this two-step positioning approach are studied in detail.

A. Estimation of Position Related Parameters

As shown in Fig. 4(b), the first step in a two-step positioning algorithm involves the estimation of parameters related to the position of the target node. Those parameters are usually related to the energy, timing, and/or direction of the signals traveling between the target node and the reference nodes. Although it is common to estimate a single parameter for each signal between the target node and a reference node, such as the arrival time of the signal, it is also possible to estimate multiple position related parameters per signal in order to improve positioning accuracy.

1) Received Signal Strength: As the energy of a signal changes with distance, the RSS at a node conveys information about the distance ("range") between that node and the node that has transmitted the signal. In order to convert the RSS information into a range estimate, the relation between distance and signal energy should be known. In the presence of such a relation, the distance between the nodes can be estimated from the RSS measurement at one of the nodes assuming that the transmitted signal energy is known.

One factor that affects the signal energy is called *path loss*, which refers to the reduction of signal power/energy as it propagates through space. A common model for path loss is given by

$$\bar{P}(d) = P_0 - 10n\log_{10}(d/d_0) \tag{6}$$

where n is called the *path-loss exponent*, $\bar{P}(d)$ is the average received power in decibels at a distance d, and P_0 is the received power in decibels at a short reference distance d_0. The relation in (6) specifies the relation between the power loss and distance through the path-loss exponent.

Although there is a simple relation between *average* signal power and distance as shown in (6), the exact relation between distance and signal energy in a practical wireless environment is quite complicated due to propagation mechanisms such as reflection, scattering, and diffraction, which can cause significant fluctuations in RSS even over short distances and/or small time intervals. In order to obtain a reliable range estimate, signal power is commonly obtained as

$$P(d) = \frac{1}{T}\int_0^T |r(t,d)|^2 dt \tag{7}$$

where $r(t,d)$ is the received signal at distance d and T is the integration interval. Although the averaging operation in (7) can mitigate the short-term fluctuations called *small-scale fading*, the average power (or RSS) still varies about its local mean, given by (6), due to *shadowing* effects, which represent signal energy variations due to the obstacles in the environment. Shadowing is commonly modeled by a zero-mean Gaussian random variable in the logarithmic scale. Therefore, the received power $P(d)$ in decibels can be expressed as[3]

$$P(d) \sim \mathcal{N}\left(\bar{P}(d), \sigma_{\text{sh}}^2\right) \tag{8}$$

where $\bar{P}(d)$ is as given in (6) and σ_{sh}^2 is the variance of the log-normal shadowing variable.

From (8), it is observed that accurate knowledge of the path-loss exponent and the shadowing variance is required

[3]There is also thermal noise in practical systems, which can be location-dependent. In this paper, it is assumed that the thermal noise is sufficiently mitigated [21].

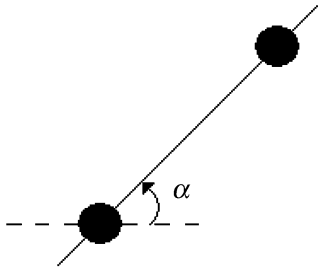

Fig. 5. *The AOA measurement at a node gives information about the direction over which the target node lies.*

for a reliable range estimate based on RSS measurements. How accurate a range estimate can be obtained is specified by a lower bound, called the Cramer–Rao lower bound (CRLB), on the variance of an unbiased[4] range estimate [21]

$$\sqrt{\mathrm{Var}\{\hat{d}\}} \geq \frac{(\ln 10)\sigma_{\mathrm{sh}} d}{10n} \tag{9}$$

where $\hat{d}$ represents an unbiased estimate for the distance d. Note from (9) that the range estimates get more accurate as the standard deviation of the shadowing decreases, which makes RSS vary less around the true average power. Also, a larger path-loss exponent results in a smaller lower bound, since the average power becomes more sensitive to distance for larger n. Finally, the accuracy of the range estimates deteriorates as the distance between the nodes increases.

Commonly, the RSS technique cannot provide very accurate range estimates due to its heavy dependence on the channel parameters, which is also true for UWB systems. For example, in a non-line-of-sight (NLOS) residential environment, modeled according to the IEEE 802.15.4a UWB channel model [22], with $n = 4.58$ and $\sigma_{\mathrm{sh}} = 3.51$, the lower bound in (9) is about 1.76 m. at $d = 10$ m.

2) Angle of Arrival: Another position related parameter is AOA, which specifies the angle between two nodes as shown in Fig. 5. Commonly, multiple antennas in the form of an antenna array are employed at a node in order to estimate the AOA of the signal arriving at that node. The main idea behind AOA estimation via antenna arrays is that differences in arrival times of an incoming signal at different antenna elements contain the angle information for a known array geometry [17]. For example, in a uniform linear array (ULA) configuration, as shown in Fig. 6, the incoming signal arrives at consecutive array elements with $l\sin\alpha/c$ seconds difference,[5] where l is the interelement spacing, α is the AOA, and c represents the speed of light [2]. Hence, estimation of the time differences of arrivals provides the angle information.

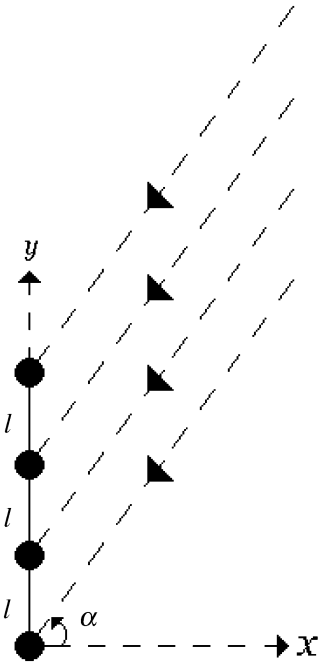

Fig. 6. *A ULA configuration and a signal arriving at the ULA with angle* α.

Since time delay in a narrow-band signal can be approximately represented by a phase shift, the combinations of the phase-shifted versions of received signals at array elements can be tested for various angles in order to estimate the direction of signal arrival [23] in a narrow-band system. However, for UWB systems, time-delayed versions of received signals should be considered, because a time delay cannot be represented by a unique phase value for a UWB signal.

Similar to the RSS case, the theoretical lower bounds on the error variances of AOA estimates can be investigated in order to determine accuracy of AOA estimation. The CRLB for the variance of an unbiased AOA estimate $\hat{\alpha}$ for a ULA with N_{a} elements can be expressed as[6] [24]

$$\sqrt{\mathrm{Var}\{\hat{\alpha}\}} \geq \frac{\sqrt{3}c}{\sqrt{2}\pi\sqrt{\mathrm{SNR}}\beta\sqrt{N_{\mathrm{a}}\left(N_{\mathrm{a}}^2-1\right)}l\cos\alpha} \tag{10}$$

where α is the AOA, c is the speed of light, SNR is the signal-to-noise ratio for each element,[7] l is the interelement spacing, and β is the effective bandwidth.

[4]For an unbiased estimate, the mean (expected value) of the estimate is equal to the true value of the parameter to be estimated.

[5]It is assumed that the distance between the transmitting and receiving nodes are sufficiently large so that the incoming signal can be modeled as a planar wave-front as shown in Fig. 6.

[6]It is assumed that the signal arrives at each antenna element via a single path. Please refer to [24] for CRLBs for AOA estimation in multipath channels.

[7]The same SNR is assumed for all antenna elements.

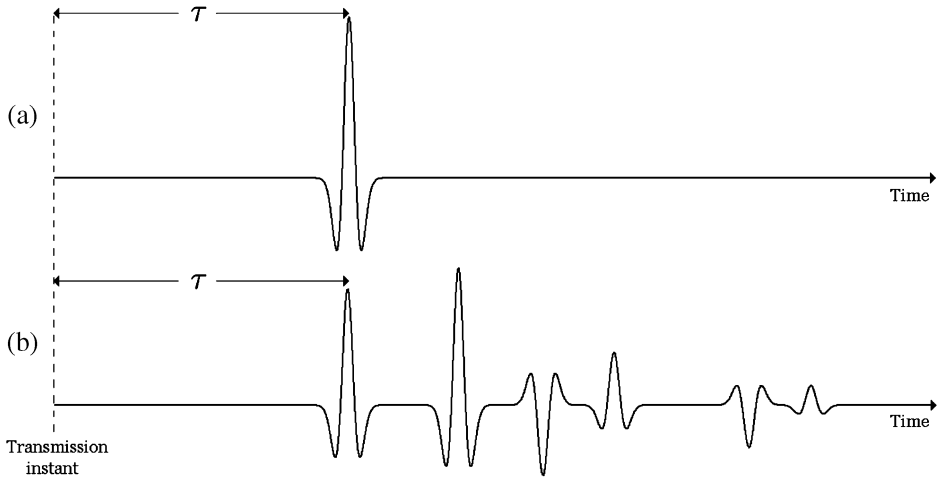

Fig. 7. *(a) Received signal in a single-path channel. (b) Received signal over a multipath channel. Noise is not shown in the figure.*

It is observed from (10) that the accuracy of AOA estimation increases as SNR, effective bandwidth, the number of antenna elements, and/or interelement spacing are increased. It is important to note that unlike RSS estimates, the accuracy of an AOA estimate increases linearly with the effective bandwidth, which implies that UWB signals can facilitate high-precision AOA estimation.

3) Time of Arrival: The TOA of a signal traveling from one node to another can be used to estimate the distance between those two nodes. In order to obtain an unambiguous TOA estimate, the nodes must either have a common clock or exchange timing information by certain protocols such as a two-way ranging protocol [3], [25], [26].

The conventional TOA estimation technique involves the use of correlator or matched filter (MF) receivers [27]. In order to illustrate the basic principle behind these receivers, consider a scenario in which $s(t)$ is transmitted from one node to another, and the received signal is expressed as

$$r(t) = s(t-\tau) + n(t) \tag{11}$$

where τ is the TOA and $n(t)$ is the background noise, which is commonly modeled as a zero-mean white Gaussian process. A correlator receiver correlates the received signal $r(t)$ with a local template $s(t-\hat{\tau})$ for various delays $\hat{\tau}$ and calculates the delay corresponding to the correlation peak; that is

$$\hat{\tau}_{\mathrm{TOA}} = \arg\max_{\hat{\tau}} \int r(t)s(t-\hat{\tau})dt. \tag{12}$$

It is clear from (11) and (12) that the correlator output is maximized at $\hat{\tau} = \tau$ in the absence of noise. However, the presence of noise can result in erroneous TOA estimates.

Similar to the correlator receiver, the MF receiver employs a filter that is matched to the transmitted signal and estimates the instant at which the filter output attains its largest value, which results in (12) as well. Both the correlator and the MF approaches are optimal[8] for the signal model in (11) [Fig. 7(a)]. However, in practical systems, the signal arrives at the receiver via multiple signal paths, as shown in Fig. 7(b). In those cases, the optimal template signal for a correlator receiver (or the optimal impulse response for an MF receiver) should include the overall effects of the channel; that is, it should be equal to the received signal (with no noise) that consists of all incoming signal paths. Since the parameters of the multipath channel are not known at the time of TOA estimation, the conventional schemes use the transmitted signal as the template, which makes them suboptimal in general. In this case, selection of the correlation peak as in (12) can result in significant errors, as the first signal path may not be the strongest signal one, as shown in Fig. 7(b). In order to achieve accurate TOA estimation in multipath environments, first-path detection algorithms are proposed for UWB systems [25], [29]–[31], which try to select the first incoming signal path instead of the strongest one.

Accuracy limits for TOA estimation can be quantified by the CRLB, which is given by the following[9] for the signal model in (11)

$$\sqrt{\mathrm{Var}(\hat{\tau})} \geq \frac{1}{2\sqrt{2}\pi\sqrt{\mathrm{SNR}\beta}} \tag{13}$$

[8]In the sense that they achieve the CRLB for TOA estimation asymptotically for large SNRs and/or effective bandwidths [28].

[9]The CRLBs for TOA estimation in multipath channels are studied in [10], [32].

where $\hat{\tau}$ represents an unbiased TOA estimate, SNR is the signal-to-noise ratio, and β is the effective bandwidth [33], [34]. The CRLB expression in (13) implies that the accuracy of TOA estimation increases with SNR and effective bandwidth. Therefore, large bandwidths of UWB signals can facilitate very precise TOA measurements. As an example, for the second derivative of a Gaussian pulse [35] with a pulse width of 1 ns, the CRLB for the standard deviation of an unbiased range estimate (obtained by multiplying the TOA estimate by the speed of light) is less than a centimeter at an SNR of 5 dB.

4) Time Difference of Arrival: Another position-related parameter is the difference between the arrival times of two signals traveling between the target node and two reference nodes. This parameter, called time difference of arrival (TDOA), can be estimated unambiguously if there is synchronization among the reference nodes [23].

One way to estimate TDOA is to obtain TOA estimates related to the signals traveling between the target node and two reference nodes and then to obtain the difference between those two estimates. Since the reference nodes are synchronized, the TOA estimates contain the same timing offset (due to the asynchronism between the target node and the reference nodes). Therefore, the offset terms cancel out as the TDOA estimate is obtained as the difference between the TOA estimates [17].

When the TDOA estimates are obtained from the TOA estimates as described above, the accuracy limits can be deduced from the CRLB expression in the previous section. Namely, it can be concluded that the accuracy of TDOA estimation improves as effective bandwidth and/or SNR increases [17].

Another way to obtain the TDOA parameter is to perform cross-correlations of the two signals traveling between the target node and the reference nodes and to calculate the delay corresponding to the largest cross-correlation value [36]. That is

$$\hat{\tau}_{\mathrm{TDOA}} = \arg\max_{\tau} \left| \int_0^T r_1(t) r_2(t+\tau) dt \right| \qquad (14)$$

where $r_i(t)$, for $i = 1, 2$, represents the signal traveling between the target node and the ith reference node and T is the observation interval.

5) Other Position-Related Parameters: In some positioning systems, a combination of position-related parameters, studied in the previous sections, can be utilized in order to obtain more information about the position of the target node. Examples of such *hybrid* schemes include TOA/AOA [37], TOA/RSS [38], TDOA/AOA [37], and TOA/TDOA [39] positioning systems.

In addition to the algorithms that estimate RSS, AOA, and T(D)OA parameters or their combinations, another scheme for position-related parameter estimation involves measurement of multipath power delay profile (PDP)[10] or channel impulse response (CIR) related to a received signal [40]–[43]. In certain cases, PDP or CIR parameters can provide significantly more information about the position of the target node than the previously studied schemes [17]. For example, a single TOA measurement provides information about the distance between a target and a reference node, which determines the position of the target on a circle; however, CIR information can directly determine the position of the target node in certain cases if the observed channel profile is unique for the given environment. In order to obtain position estimates from CIR (or PDP) parameters, a database consisting of previous PDP (or CIR) measurements at a number of known positions is commonly required. In addition, estimation of PDP/CIR information is usually more complex than the estimation of the previously studied parameters [2].

B. Position Estimation

As shown in Fig. 4(b), in the second step of a two-step positioning algorithm, the position of the target node is estimated based on the position-related parameters estimated in the first step. Depending on the presence of a database (training data), two types of position estimation schemes can be considered [17].

- *Geometric* and *statistical* techniques estimate the position of the target node from the signal parameters, estimated in the first step of the positioning algorithm, via geometric relationships and statistical approaches, respectively.
- *Mapping (fingerprinting)* techniques employ a database, which consists of previously estimated signal parameters at known positions, to estimate the position of the target node. Commonly, the database is obtained beforehand by a training (offline) phase.

1) Geometric and Statistical Techniques: Geometric techniques for position estimation determine the position of a target node according to geometric relationships. For example, a TOA (or an RSS) measurement specifies the range between a reference node and a target node, which defines a circle for the possible positions of the target node. Therefore, in the presence of three measurements, the position of the target node can be determined by the intersection of three circles[11] via *trilateration*, as shown in Fig. 8. On the other hand, two AOA measurements between a target node and two reference nodes can be used to determine the position of the target node via

[10]Similar to the PDP parameter, the multipath angular power profile parameter can be estimated at nodes with antenna arrays.

[11]A two-dimensional positioning scenario is considered for the simplicity of illustrations.

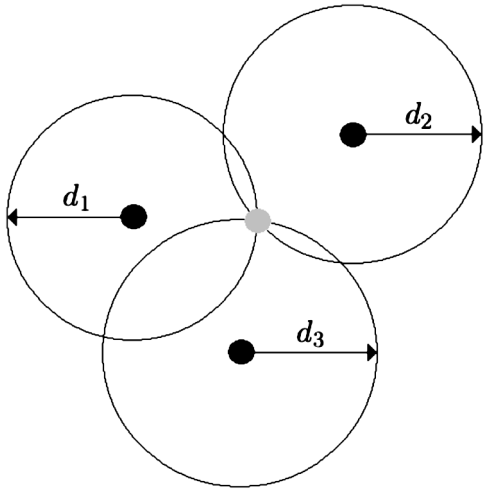

Fig. 8. ***Position estimation via trilateration.***

triangulation (Fig. 9). For TDOA-based positioning, each TDOA parameter defines a hyperbola for the position of the target node. Hence, in the presence of three reference nodes, two TDOA measurements can be obtained with respect to one of the reference nodes. Then, the intersection of two hyperbolas, corresponding to two TDOA measurements, determines the position of the target node as shown in Fig. 10. In TDOA-based positioning, the position of the target node may not always be determined uniquely depending on the geometrical conditioning of the nodes [23], [44].

Geometric techniques can be employed for hybrid positioning systems, such as TDOA/AOA [37] or TOA/TDOA [39], as well. For example, if a reference node obtains both TOA and AOA parameters from a target node, it can determine the position of the target node as the intersection of a circle, defined by the TOA parameter, and a straight line, defined by the AOA parameter [17].

Although the geometric techniques provide an intuitive approach for position estimation in the absence of noise,

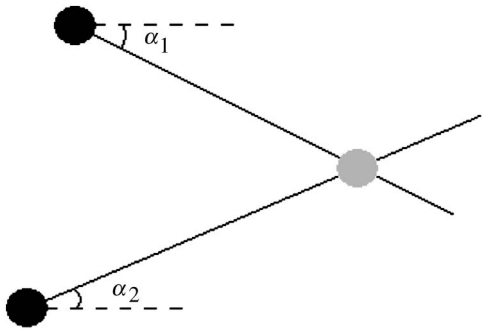

Fig. 9. ***Position estimation via triangulation.***

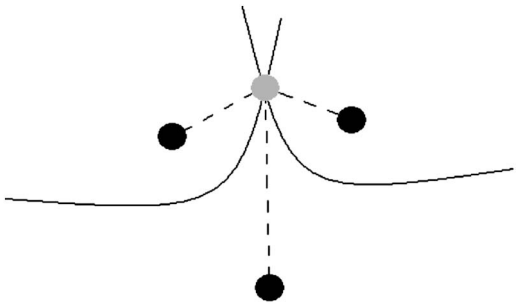

Fig. 10. ***Position estimation based on TDOA measurements.***

they do not present a systematic approach for position estimation based on noisy measurements. In practice, position-related parameter measurements include noise, which results in the cases that the position lines intersect at multiple points, instead of a single point, as shown in Fig. 11. In such cases, the geometric techniques do not provide any insight as to which point to choose as the position of the target node [2]. In addition, as the number of reference nodes increases, the number of intersections can increase even further. In other words, the geometric techniques do not provide an efficient data fusion mechanism; i.e., cannot utilize multiple parameter estimates in an efficient manner [17].

Unlike the geometric techniques, the statistical techniques present a theoretical framework for position estimation in the presence of multiple position-related parameter estimates with or without noise. To formulate this generic framework, consider the following model for

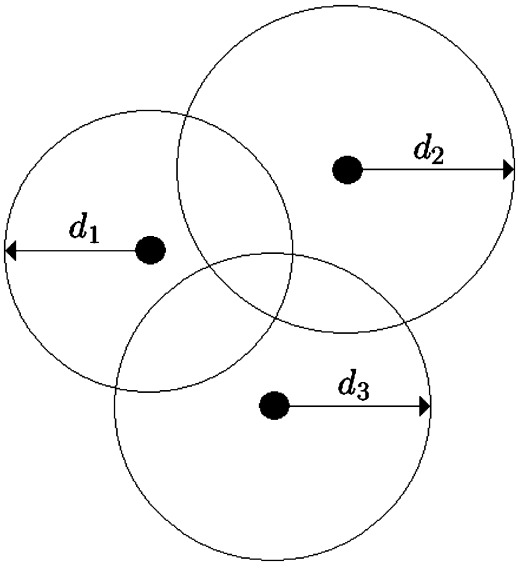

Fig. 11. ***Position estimation ambiguities due to multiple intersections of position lines.***

the parameters obtained from the first step of a two-step positioning algorithm [17]:

$$z_i = f_i(x,y) + \eta_i, \quad i = 1, \ldots, N_m \tag{15}$$

where N_m is the number of parameter estimates, $f_i(x,y)$ is the true value of the ith signal parameter, which is a function of the position of the target (x,y), and η_i is the noise at the ith estimation. Note that N_m is equal to the number of reference nodes for RSS-, AOA-, and TOA-based positioning, whereas it is one less than the number of reference nodes for TDOA-based positioning since each TDOA parameter is estimated with respect to one reference node. Depending on the type of the position-related parameter, $f_i(x,y)$ in (15) can be expressed as[12]

$$f_i(x,y) = \begin{cases} \sqrt{(x-x_i)^2 + (y-y_i)^2}, & \text{TOA/RSS} \\ \tan^{-1}\left(\frac{y-y_i}{x-x_i}\right), & \text{AOA} \\ \sqrt{(x-x_i)^2 + (y-y_i)^2} & \\ \quad - \sqrt{(x-x_0)^2 + (y-y_0)^2}, & \text{TDOA} \end{cases} \tag{16}$$

where (x_i, y_i) is the position of the ith reference node and (x_0, y_0) is the reference node, relative to which the TDOA parameters are estimated.

In vector notations, the model in (15) can be expressed as

$$\mathbf{z} = \mathbf{f}(x,y) + \boldsymbol{\eta} \tag{17}$$

where $\mathbf{z} = [z_1 \cdots z_{N_m}]^T$, $\mathbf{f}(x,y) = [f_1(x,y) \cdots f_{N_m}(x,y)]^T$ and $\boldsymbol{\eta} = [\eta_1 \cdots \eta_{N_m}]^T$.

A statistical approach estimates the most likely position of the target node based on the reliability of each parameter estimate, which is determined by the characteristics of the noise corrupting that estimate. Depending on the amount of information on the noise term $\boldsymbol{\eta}$ in (17), the statistical techniques can be classified as *parametric* and *nonparametric* techniques [2]. For the parametric techniques, the probability density function (pdf) of the noise $\boldsymbol{\eta}$ is known except for a set of parameters, denoted by $\boldsymbol{\lambda}$. However, for the nonparametric techniques, there is no information about the form of the noise pdf. Although the form of the pdf is unknown in the nonparametric case, there can still be some generic information about some of its parameters [45], such as its variance and symmetry properties, which can be employed for designing nonparametric estimation rules, such as the least median of squares technique in [46], the residual weighting algorithm in [47], and the variance weighted least squares technique in [48]. In addition, mapping techniques (to be studied in Section II-B2), such as k nearest neighbor (k-NN) estimation, support vector regression (SVR), and neural networks, are also nonparametric, as they estimate the position based on a training database without assuming a specific form for the noise pdf.

Considering the parametric approaches, let the vector of unknown parameters be represented by $\boldsymbol{\theta}$, which consists of the position of the target node, as well as the unknown parameters of the noise distribution;[13] i.e., $\boldsymbol{\theta} = [x\ y\ \boldsymbol{\lambda}^T]^T$. Depending on the availability of prior information on $\boldsymbol{\theta}$, Bayesian or maximum likelihood (ML) estimation techniques can be applied [49].

For the Bayesian approach, there exists *a priori* information on $\boldsymbol{\theta}$, represented by a prior probability distribution $\pi(\boldsymbol{\theta})$. A Bayesian estimator obtains an estimate of $\boldsymbol{\theta}$ by minimizing a specific cost function [33]. Two common Bayesian estimators are the minimum mean square error (MMSE) and the maximum *a posteriori* (MAP) estimators,[14] which estimate $\boldsymbol{\theta}$, respectively, as

$$\hat{\boldsymbol{\theta}}_{\text{MMSE}} = \text{E}\{\boldsymbol{\theta}|\mathbf{z}\} \tag{18}$$

$$\hat{\boldsymbol{\theta}}_{\text{MAP}} = \arg\max_{\boldsymbol{\theta}} p(\mathbf{z}|\boldsymbol{\theta})\pi(\boldsymbol{\theta}) \tag{19}$$

where $\text{E}\{\boldsymbol{\theta}|\mathbf{z}\}$ is the conditional expectation of $\boldsymbol{\theta}$ given $\mathbf{z}$ and $p(\mathbf{z}|\boldsymbol{\theta})$ represents the conditional pdf of $\mathbf{z}$ given $\boldsymbol{\theta}$ [17].

For the ML approach, there is no prior information on $\boldsymbol{\theta}$. In this case, an ML estimator calculates the value of $\boldsymbol{\theta}$ that maximizes the likelihood function $p(\mathbf{z}|\boldsymbol{\theta})$; i.e.,

$$\hat{\boldsymbol{\theta}}_{\text{ML}} = \arg\max_{\boldsymbol{\theta}} p(\mathbf{z}|\boldsymbol{\theta}). \tag{20}$$

Since $\mathbf{f}(x,y)$ is a deterministic function, the likelihood function can be expressed as

$$p(\mathbf{z}|\boldsymbol{\theta}) = p_{\boldsymbol{\eta}}(\mathbf{z} - \mathbf{f}(x,y)|\boldsymbol{\theta}) \tag{21}$$

where $p_{\boldsymbol{\eta}}(\cdot|\boldsymbol{\theta})$ denotes the conditional pdf of the noise vector given $\boldsymbol{\theta}$.

In statistical approaches, the exact form of the position estimator depends on the noise statistics. An example is studied below [2].

[12]Time parameters are converted to distance parameters by scaling by the speed of light.

[13]In general, the noise components may also depend on the position of the target node, in which case $\boldsymbol{\theta}$ includes the union of x, y and the elements in $\boldsymbol{\lambda}$.

[14]Although MAP estimation is not properly a Bayesian approach, it still fits within the Bayesian framework [33].

Example 1: Assume that the noise components are independent. Then, the likelihood function in (21) can be expressed as

$$p(\mathbf{z}|\boldsymbol{\theta}) = \prod_{i=1}^{N_m} p_{\eta_i}(z_i - f_i(x,y)|\boldsymbol{\theta}) \tag{22}$$

where $p_{\eta_i}(\cdot|\boldsymbol{\theta})$ represents the conditional pdf of the ith noise component given $\boldsymbol{\theta}$. In addition, if the noise pdfs are given by zero-mean Gaussian random variables

$$p_{\eta_i}(n) = \frac{1}{\sqrt{2\pi}\sigma_i} \exp\left(-\frac{n^2}{2\sigma_i^2}\right) \tag{23}$$

for $i = 1, \ldots, N_m$, with known variances, the likelihood function in (22) becomes

$$p(\mathbf{z}|\boldsymbol{\theta}) = \frac{1}{(2\pi)^{N_m/2} \prod_{i=1}^{N_m} \sigma_i} \times \exp\left(-\sum_{i=1}^{N_m} \frac{(z_i - f_i(x,y))^2}{2\sigma_i^2}\right) \tag{24}$$

where the unknown parameter vector $\boldsymbol{\theta}$ is given by $\boldsymbol{\theta} = [x\ y]^T$. In the absence of any prior information on $\boldsymbol{\theta}$, the ML approach can be followed, and the ML estimator in (20) can be obtained from (24) as

$$\hat{\boldsymbol{\theta}}_{ML} = \arg\min_{[x\ y]^T} \sum_{i=1}^{N_m} \frac{(z_i - f_i(x,y))^2}{\sigma_i^2} \tag{25}$$

which is the well-known nonlinear least squares (NLS) estimator [17], [23]. Note that the terms in the summation are weighted inversely proportional to the noise variances, as a larger variance means a less reliable estimate. Among common techniques for solving (25) are gradient descent algorithms and linearization techniques via the Taylor series expansion [23], [50].

In Example 1, the noise components related to different estimates are assumed to be independent. This assumption is usually valid for TOA, RSS, and AOA estimation. However, for TDOA estimation, the noise components are correlated, since all TDOA parameters are obtained with respect to the same reference node. Therefore, TDOA-based systems should be studied through the generic expression in (21). In addition, the Gaussian model for the noise terms is not always very accurate, especially for scenarios in which there is no direct propagation path between the target node and the reference node. For such NLOS situations, position estimation can be quite challenging, as will be discussed in Section III-A3.

3) Mapping Techniques: A mapping technique utilizes a training data set to determine a position estimation rule (pattern matching algorithm/regression function) and then uses that rule in order to estimate the position of a target node for a given set of position related parameter estimates. Common mapping techniques include k-NN, SVR, and neural networks [43], [51]–[55].

Consider a training data set given by

$$\mathcal{T} = \{(\mathbf{m}_1, \boldsymbol{l}_1), (\mathbf{m}_2, \boldsymbol{l}_2), \ldots (\mathbf{m}_{N_T}, \boldsymbol{l}_{N_T})\} \tag{26}$$

where $\mathbf{m}_i$ represents the vector of estimated parameters (measurements) for the ith position, $\boldsymbol{l}_i$ is the position (location) vector for the ith training data, which is given by $\boldsymbol{l}_i = [x_i\ y_i]^T$ for two-dimensional positioning, and N_T is the total number of elements in the training set [17]. Depending on the type of the position-related parameters employed in the system, $\mathbf{m}_i$ can, for example, consist of RSS parameters measured at the reference nodes when the target node is at location $\boldsymbol{l}_i$. A mapping technique determines a position estimation rule based on the training set in (26) and then estimates the position of a target node by using that estimation rule with the measurements related to the target node.

In order to provide intuition on mapping techniques for position estimation, the k-NN approach can be considered. Let $\boldsymbol{l}$ denote the position of a target node and $\mathbf{m}$ the measurements (parameter estimates) related to that node. The k-NN scheme estimates the position of the target node according to the k parameter vectors in $\mathcal{T}$ that have the smallest Euclidian distances to the given parameter vector $\mathbf{m}$. The position estimate $\hat{\boldsymbol{l}}$ is calculated as the weighted sum of the positions corresponding to those nearest parameter vectors; i.e.,

$$\hat{\boldsymbol{l}} = \sum_{i=1}^{k} w_i(\mathbf{m}) \boldsymbol{l}^{(i)} \tag{27}$$

where $\boldsymbol{l}^{(1)}, \ldots, \boldsymbol{l}^{(k)}$ are the positions corresponding to the k nearest parameter vectors, $\mathbf{m}^{(1)}, \ldots, \mathbf{m}^{(k)}$, to $\mathbf{m}$, and $w_1(\mathbf{m}), \ldots, w_k(\mathbf{m})$ are the weighting factors for each position. In general, the weighting factors are determined according to the parameter vector $\mathbf{m}$ and the training parameter vectors $\mathbf{m}^{(1)}, \ldots, \mathbf{m}^{(k)}$ [51].

SVR and neural network approaches can also be considered in the same framework as the k-NN technique [55]. For example, SVR estimates the position also based on a weighted sum of the positions in the training set. However, the weights are chosen in order to minimize a risk function that is a combination of empirical error and regressor complexity. Minimization of the empirical error

corresponds to fitting to the data in the training set as well as possible, while a constraint on the regressor complexity prevents the overfitting problem [56]. In other words, the SVR technique considers the tradeoff between the empirical error and the generalization error.[15]

In addition to k-NN and SVR, neural networks can also be employed in position estimation problems [43], [57]. In [57], a UWB mapping technique based on neural networks is proposed in order to provide accurate position estimation in mines. In general, in challenging environments, like mines, measurement models become less reliable; hence position estimation based on statistical approaches can result in large errors. Therefore, the mapping techniques can be preferred in the absence of reliable signal modeling. They can provide accurate position estimation in environments with significant multipath and NLOS propagation.

The main limitation of the mapping techniques compared to statistical and geometric ones is that the training data set should be large enough and representative of the current environment. In other words, the training set should be updated at sufficient frequency, which can be very costly in dynamic environments. Therefore, mapping techniques are not commonly employed in outdoor positioning scenarios.

In terms of accuracy, performance of the mapping techniques compared to the geometric and the statistical techniques depends on the environment and system parameters. The most important parameters in a mapping technique are the size and the representativeness of the training set and the accuracy of the regression technique. On the other hand, geometric and statistical techniques require accurate signal (measurement) models in order to provide accurate position estimates.

III. TIME-BASED RANGING

In a two-step positioning algorithm, the positioning accuracy increases as the position-related parameters in the first step are estimated more precisely. As studied in Section II-A, high time resolution of UWB signals can facilitate precise T(D)OA or AOA estimation; however, RSS estimation provides very coarse range estimates as observed in Section II-A1. In addition, AOA estimation commonly requires multiple antenna elements and increases the complexity of a UWB receiver. Therefore, timing-related parameters, especially TOA, are commonly preferred for UWB positioning systems.

In this section, TOA estimation is studied in detail. First, main sources of errors in TOA estimation are investigated for practical UWB positioning systems, and then common TOA estimation techniques are reviewed. As TOA information can be used to obtain the distance, commonly called "range," between two nodes, TOA estimation and range estimation (or ranging) will be used interchangeably in the remainder of this paper.

[15]Very complex regressors fit the training data very closely and therefore may not fit to new measurements very well, especially for small training data sets. This is called the generalization (overfitting) problem.

A. Main Sources of Errors

In a single-path propagation environment with no interfering signals and no obstructions in between the nodes, extremely accurate TOA estimation can be performed. However, in practical environments, signals arrive at a receiver via multiple signal paths, and there are interfering signals and obstructions in the environment. In addition, high time resolution of UWB signals, which facilitates accurate TOA estimation, can cause practical difficulties. Those error sources for practical TOA estimation are studied in the following sections.

1) Multipath Propagation: In a multipath environment, a transmitted signal arrives at the receiver via multiple signal paths, as shown in Fig. 7. Due to high resolution of UWB signals, pulses received via multiple paths are usually resolvable at the receiver. However, for narrow-band systems, pulses received via multiple paths overlap with each other as the pulse duration is considerably larger than the time delays between the multipath components. This causes a shift in the delay corresponding to the correlation peak [see (12)] and can result in erroneous TOA estimation. In order to mitigate those errors, superresolution time-delay estimation algorithms, such as that described in [58], were studied for narrow-band systems. However, high time resolution of UWB signals facilitates accurate correlation-based TOA estimation without the use of such complex algorithms. As discussed in Section II-A3, first-path detection algorithms can be employed for UWB systems [25], [29]–[31] in order to accurately estimate TOA by determining the delay of the first incoming signal path.

In order to analyze the effects of multipath propagation on TOA estimation, accurate characterization of UWB channels is needed [22], [59]–[62]. The UWB channel models proposed by the IEEE 802.15.4a channel modeling committee provide statistical information on delays and amplitudes of various signal paths arriving at a UWB receiver [22]. Based on that statistical information or experimental data, TOA estimation errors can be modeled [59], [60]. In [59], indoor UWB channel measurements are used to propose a statistical model for TOA estimation errors. On the other hand, [60] characterizes the statistical behavior of delay between the first and the strongest signal paths, which is an important parameter for TOA estimation, based on the IEEE 802.15.4a channel models.

2) Multiple-Access Interference: In the presence of multiple users in a given environment, signals can interfere with each other, and the accuracy of TOA estimation can degrade. A common way to mitigate the effects of multiple-access interference (MAI) is to assign different time slots or frequency bands to different users in a network. However, there can still be interference among networks that

operate at the same time intervals and/or frequency bands. Therefore, various MAI mitigation techniques, such as nonlinear filtering [63] and training sequence design [31], are commonly employed.

3) Non-Line-of-Sight Propagation: When the direct line-of-sight (LOS) between two nodes is obstructed, the direct signal component is attenuated significantly such that it becomes considerably weaker than some other multipath components, or it cannot even be detected by the receiver [59], [61], [64]. For the former case, first-path detection algorithms can still be utilized in some cases to estimate the TOA accurately. However, in the latter case, the delay of the first detectable signal path does not represent the true TOA, as it includes a positive bias, called NLOS error. Mitigation of NLOS errors is one of the most challenging tasks in accurate TOA estimation.

In order to facilitate accurate positioning in NLOS environments, mapping techniques discussed in Section II-B2 can be employed. As the training data set obtained from the environment implicitly contains information about NLOS propagation, mapping techniques have a certain degree of robustness against NLOS errors.

In the presence of statistical information about NLOS errors, various NLOS identification and mitigation algorithms can be employed [10], [59]. For example, in [65], the observation that the variance of TOA measurements in the NLOS case is usually considerably larger than that in the LOS case is used in order to identify NLOS situations, and then a simple LOS reconstruction algorithm is employed to reduce the positioning error. In addition, statistical techniques are studied in [66] and [67] in order to classify a set of measurements as LOS or NLOS. Finally, based on various scattering models for a given environment, the statistics of TOA measurements can be obtained, and then well-known techniques, such as MAP and ML, can be employed to mitigate the effects of NLOS errors [49], [68].

4) High Time Resolution of UWB Signals: Although high time resolution of UWB signals results in very precise TOA estimation, it also poses certain practical challenges. First, clock jitter becomes a significant factor that affects the accuracy of UWB positioning systems [69]. Due to short durations of UWB pulses, clock inaccuracies and drifts in target and reference nodes can affect the TOA estimates.

In addition, high time resolution of UWB signals makes it quite impractical to sample received signals at or above the Nyquist rate,[16] which is typically on the order of a few gigahertz. Therefore, TOA estimation schemes should make use of low-rate samples in order to facilitate low-power designs.

Finally, high time resolution of UWB signals results in a TOA estimation scenario, in which a large number of possible delay positions need to be searched in order to determine the true TOA. Therefore, conventional correlation-based approaches that search this delay space in a serial fashion become impractical for UWB signals. Therefore, fast TOA estimation algorithms, as will be discussed in the next section, are required in order to obtain TOA estimates in reasonable time intervals.

[16]The Nyquist rate is equal to twice the highest frequency component contained within a signal.

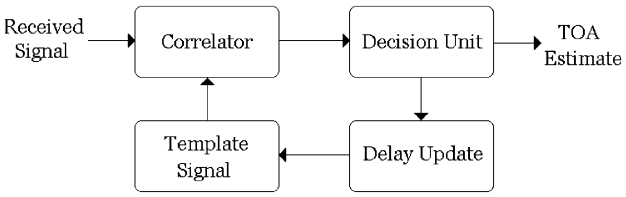

Fig. 12. *A receiver architecture for correlation-based TOA estimation.*

B. Ranging Algorithms

As discussed in Section II-A3, a conventional correlation-based TOA estimation (equivalently, ranging) algorithm correlates the received UWB signal with various delayed versions of a template signal, and obtains the TOA estimate as the delay corresponding to the correlation peak (Fig. 12). However, in practice, there is a large number of possible signal delays that need to be searched for the correlation peak due to high time resolution of UWB signals, and also the correlation peak may not always correspond to the true TOA. Therefore, a serial search strategy can be employed, which estimates the delay corresponding to the first correlation output that exceeds a certain threshold [23], [29], [70]. However, also the serial search approach can take a very long time to obtain a TOA estimate in many cases [71]. In order to speed up the estimation process, different search strategies, such as random search or bit reversal search, can be employed [72]. For example, in a random search strategy, possible signals delays are selected randomly and tested for the TOA. In the presence of multipath propagation, the random search strategy can reduce the time to obtain a rough TOA estimate; that is, to determine the delay of a signal path (not necessarily the first one). Then, fine TOA estimation can be performed by searching backwards in time from the detected signal component [73].

In general, two-step approaches that estimate a rough TOA in the first step and then obtain a fine TOA estimate in the second step can provide significant reduction in the amount of time to perform ranging [30]. Commonly, rough TOA estimation in the first step can be performed by low-complexity receivers rapidly, which considerably reduces the possible delay positions that need to be searched for the fine TOA in the second step. For example, in [30], a simple energy detector is employed for determining a rough TOA estimation; i.e., for reducing the TOA search space. Then, the second step searches for the TOA within a

smaller interval determined by the first step. For the second step, correlation-based first-path detection schemes [25], [29] or statistical change detection approaches [30] can be employed.

As discussed, in Section III-A4, TOA estimation based on low-rate sampling, compared to the Nyquist rate sampling, is desirable for low-power implementations. Examples of such low-rate TOA estimators include ones that employ energy detectors (noncoherent receivers), low-rate correlator outputs, or symbol rate autocorrelation receivers [31], [74]–[76].

IV. PRACTICAL CONSIDERATIONS

After studying theoretical aspects and estimation algorithms for UWB positioning and ranging systems, we now consider practical issues related to the design of UWB ranging signals, and hardware issues for UWB transmitters and receivers.

A. Signal Design

In order to meet certain performance requirements under practical and regulatory constraints, UWB ranging signals should be designed appropriately [2]. The main performance criterion in a ranging system is ranging accuracy, which is commonly quantified by the root mean square error (RMSE) given by

$$\mathrm{RMSE} = \sqrt{\mathrm{E}\{(\hat{d} - d)^2\}} \tag{28}$$

where $\hat{d}$ is the range estimate and d is the true range. In other words, the RMSE is defined as the square root of the average value of the squared error.[17] In practice, the expected value in (28) is approximated by the sample mean of the squared error; i.e.,

$$\mathrm{RMSE} \approx \sqrt{\frac{1}{N}\sum_{i=1}^{N}(\hat{d}_i - d_i)^2} \tag{29}$$

where d_i and $\hat{d}_i$ are, respectively, the true range and the range estimate for the ith measurement, for $i = 1, \ldots, N$.

In addition to ranging accuracy, the duration of a ranging signal is another important parameter for UWB ranging systems [2]. For small durations of ranging signals, range estimates can be obtained quickly and also more signal resources can be allocated for data transmission if the system is performing both ranging and communications. Intuitively, as the duration of ranging signal increases, more accurate range (TOA) estimation can be performed. This can be observed also from the CRLB expression in (13). To that end, consider a generic ranging signal structure, as shown in Fig. 3, which is expressed as

$$s(t) = \sum_{j=-\infty}^{\infty} a_j \omega(t - jT_{\mathrm{f}}) \tag{30}$$

where $\omega(t)$ is a UWB pulse, T_{f} is the frame interval (or, pulse repetition interval), which is commonly considerably larger than the pulse width, and a_j is a binary $\{-1, +1\}$ or ternary $\{-1, 0, +1\}$ code, which is used for interference robustness and spectral optimization [77]–[79]. For example, in the IEEE 802.15.4a standard, ternary codes are employed for the synchronization preamble of each packet, which is used for ranging purposes [3].

According to the FCC regulations, as shown in Fig. 2, there is a limit on the average PSD of a UWB signal. Depending on the spectral characteristics of the signal in (30), the maximum amount of average power $P_{\max}$ that can be transmitted by a UWB transmitter can be determined from the FCC limit. Then, the maximum energy of a pulse in a frame can be calculated as $T_{\mathrm{f}}P_{\max}$. Therefore, for a ranging system that employs N_{f} UWB pulses, the SNR in the CRLB expression in (13) becomes directly proportional to $TP_{\max}$, where $T = N_{\mathrm{f}}T_{\mathrm{f}}$. Hence, as the duration of the ranging signal increases, better accuracy can be achieved; i.e., the ranging signal duration and the lower bound on the error variance of unbiased range estimators are inversely proportional.

Design of a ranging signal, as in (30), also requires an appropriate selection of the frame interval T_{f}. As studied above, the maximum energy of a pulse in a frame is proportional to the frame interval. Hence, for a given pulse width (or the signal bandwidth), the maximum peak power increases as the frame interval increases. The peak power is an important parameter in UWB ranging systems due to practical limitations of integrated circuits [80] and regulatory constraints [1]. Therefore, there exists a practical upper bound on the frame interval for UWB systems that operate at maximum power limits. On the other hand, very small frame intervals are not desirable either, as they can result in interference between pulses in consecutive frames due to the effects of multipath propagation. Also, large frame intervals can facilitate low power designs, as some units in the receiver, such as an analog-to-digital converter (ADC), can be run only when pulses arrive [81].

After determining the length of the ranging signal T and the frame interval T_{f}, another important issue is related to *pulse coding*, which is implemented by the sequence $\{a_j\}$ in (30). Pulse coding is quite important for reliable range estimation, as coded pulses in a ranging signal can provide robustness against multipath and multiple-access interference (MAI). While autocorrelation properties of a code determine its robustness against multipath interference, its cross-correlation properties

[17] A more generic accuracy metric is the cumulative distribution function (cdf) of the ranging error, which specifies the probability that the ranging error is smaller than a given threshold value for all possible thresholds.

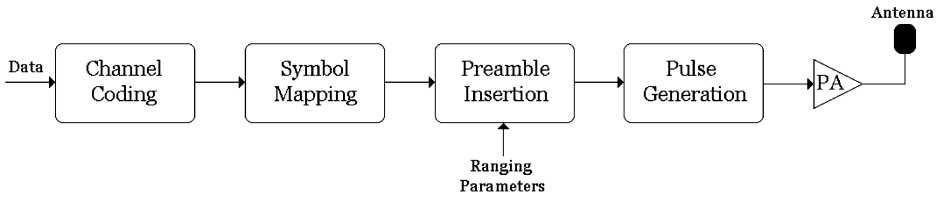

Fig. 13. *Block diagram of a UWB transmitter in a communications system with ranging capability [2].*

become effective in mitigating MAI [2]. In addition, code length is an important parameter; since better correlation properties can be obtained with longer codes, but shorter codes ease the acquisition process [77], [82].

B. Hardware Issues

After the selection of signal parameters, implementation of a UWB system requires the design of hardware components for UWB transmitters and receivers. Due to large bandwidths of UWB signals, conventional hardware design techniques are not applicable to certain sections of a UWB transmitter/receiver. In this section, various issues related to hardware design for UWB systems are briefly investigated.

UWB systems that provide ranging information commonly perform both communications and ranging, as in typical IEEE 802.15.4a systems [3]. In other words, such UWB systems provide low-to-medium rate data communications together with ranging capability. Fig. 13 illustrates the block diagram of a UWB transmitter in such a UWB system [2]. As shown in the figure, communications data are first coded in order to provide robustness against the adverse effects of the channel. In other words, some systematic redundancy is added into the data in order to recover the correct data at the receiver in the presence of errors. Then, the coded data are mapped onto specific symbols for modulation purposes. As an example, the coded data can be mapped onto binary phase-shift keying symbols, which take values from the set $\{-1, +1\}$. After symbol mapping, ranging-related information is inserted at the beginning of the communications data. Typically, transmission is performed in terms of *packets*, which contain both communications and ranging signals; i.e., a certain section of transmission is allocated for ranging signals, and the remaining is allocated for communications signals. Since ranging signals commonly constitute the beginning section of each packet, they are also called *preambles*.[18]

The digital sequence at the output of the preamble insertion block is converted into an analog UWB pulse sequence by the pulse generation block. UWB pulse generators can be broadly classified into two depending on the use of an *up-conversion* unit.[19] Those that employ an up-conversion unit first generate a pulse at baseband and then translate the frequency contents of the signal (i.e., "up-convert" it) around a desired center frequency [83]–[85]. On the other hand, some UWB pulse generators can directly generate the pulses in the desired frequency band without employing any up-conversion unit. Among such pulse generators are those that generate UWB pulses, such as the fifth derivative of a Gaussian pulse, without any filtering operations [86], [87], those that use antenna for shaping UWB pulses [88], [89], and those that employ filtering for pulse shaping [90]–[95].

After generating UWB pulses, a power amplifier (PA) can be used to increase the power of the signal delivered to the antenna. For UWB systems operating under extremely low power regulations, such as the Japanese regulations for unlicensed use of UWB systems, use of a PA may not be needed [96]. Commonly, PAs can constitute a large portion of the transmitter power consumption. Hence, it is desirable to have efficient[20] PAs in order to minimize the power consumed at a transmitter [97]–[101].

Finally, an antenna unit transmits the UWB signal into space, as shown in Fig. 13. Related to large bandwidths of UWB signals, UWB antenna design should take a number of issues into account. First, a UWB antenna should have a wide *impedance bandwidth*, which is defined as the frequency band over which there is no more than 10% signal loss due to the mismatch between the transmitter circuitry and the antenna [2]. Ideally, when there is perfect matching, an incoming signal towards the antenna is completely radiated into space. In order to obtain large impedance bandwidths for UWB antennas, various bandwidth broadening techniques are commonly employed. Among those techniques are using specific antenna geometries such as helix, biconical, and bowtie structures [102], beveling or smoothing [103]–[106], resistive loading [107], slotting (or adding a strip) [108], [109], notching, and optimizing location or structure of the antenna feed [110]–[112]. Another important issue in UWB antenna design is that a UWB antenna should radiate a pulse that is very similar to

[18]In a system that performs both communications and ranging, preamble signals are used not only for ranging but also for timing acquisition, frequency recovery, packet and frame synchronization, and channel estimation.

[19]An up-conversion unit commonly consists of a mixer and a local oscillator. The incoming signal and the signal generated by the local oscillator is multiplied using the mixer in order to perform frequency translation.

[20]*Efficiency* of a PA is defined as the ratio between the signal power delivered to the load and the total power consumed by the amplifier.

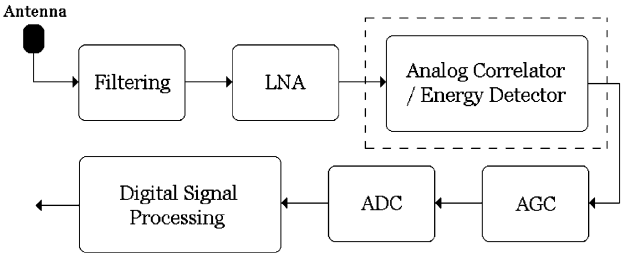

Fig. 14. ***Block diagram of a UWB receiver. The unit in the dotted box exists only when analog correlation or energy detection is to be performed [2].***

the pulse at the feed of the antenna (or its derivative) so that no significant pulse distortion occurs [107]. In addition, *radiation efficiency*, which is defined as the ratio of the radiated power to the input power at the terminals of the antenna [102], should be quite high so that there is no significant power loss. Since UWB signals operating under regulatory constraints can transmit low-power signals only, high radiation efficiency of UWB antennas is needed for ranging/communications at reasonable distances.

Commonly, planar antennas, such as bowtie, diamond, and square dipole antennas, and polygonal and elliptical monopole antennas, are well suited for UWB systems, as they are compact and can be printed on printed circuit boards ([113] and [114] and references therein). In addition, they can have wide impedance bandwidths and reasonable pulse distortion if their geometries and feeding structures are designed in an appropriate fashion [113].

Considering the receiver part, UWB signals are collected by a UWB antenna as shown in Fig. 14 [2]. Then, the signal is passed through a bandpass filter and a low-noise amplifier (LNA) for out-of-band noise/interference mitigation and signal amplification, respectively. At this point, two groups of UWB receivers can be considered. One group of UWB receivers, called "all-digital," directly convert the analog UWB signal into digital and perform all the main signal-processing operations, such as correlation, in the digital domain [115]–[117]. In other words, for all-digital UWB receivers, the units in the dotted box in Fig. 14 do not exist. On the other hand, other UWB receivers perform correlation or energy detection operations (depending on the receiver type) in the analog domain, and then perform the conversion from the analog domain to the digital domain [118]–[120]. For both receiver types, analog-to-digital conversion is performed by the ADC unit, which is preceded by the automatic gain control (AGC) that adjusts the level of the UWB signal according to ADC specifications.

An ADC obtains samples from the analog signal and quantizes those samples into a number of levels to represent a digital signal. How fast those samples are obtained *(sampling rate)*, how many bits are used to represent the digital signal *(resolution)*, and the amount of power dissipation are the main parameters of an ADC. As the sampling rate and/or the resolution increases, the complexity and the power dissipation of the ADC increases as well. Due to large bandwidths of UWB signals, design of high-speed and low-power ADCs is an important issue for UWB receivers.

For UWB receivers that perform correlation (or, energy detection) operations in the analog domain, ADCs can operate at much lower rates than the Nyquist rate, as sampling per frame or symbol becomes sufficient, which facilitates the design of low-power UWB receivers [96], [118]. However, such receivers commonly experience performance degradation due to circuit mismatches and reduced flexibility. For example, the number of correlators are usually quite limited in the analog implementation, which prevents the implementation of sophisticated narrow-band interference mitigation techniques [115].

For improved performance, it is desirable to perform analog-to-digital conversion at an early stage, as in all-digital UWB receivers. However, for those receiver, very high-speed ADCs are required, as sampling UWB signals at the Nyquist rate requires obtaining a few billion samples per second (Gsps). Fortunately, resolution requirement is not as strict as the sampling rate requirement, and an ADC with a few bits of resolution is usually sufficient for UWB signals. Specifically, an ADC with more than 4 bits of resolution provides only marginal improvement over a 4-bit ADC for UWB systems [116], [121], [122]. In order to meet the fast sampling rate requirement with the current ADC technology, various channelization techniques, such as frequency-domain channelization [115], [123]–[126] and subsampling techniques [127], [128] are commonly employed.

After the ADC, the digital signal samples are processed in order to estimate a position-related parameter, such as TOA. Then, the position-related parameters corresponding to a number of UWB nodes are used to determine the position of the target node. In self-positioning systems, the target node itself calculates the position, whereas in remote-positioning systems, a central node calculates the position of the target. In both cases, the complexity of the position estimation algorithm sets the signal-processing requirements on the related node. For example, if a mapping technique is implemented, the node needs to manage a training data set and employ it for position estimation. On the other hand, a statistical technique does not require training data management but may need to solve an optimization problem, such as the NLS algorithm in (25).

V. CONCLUSION

In this paper, we have reviewed the problem of position estimation in UWB wireless systems. We have considered primarily a two-step positioning approach, in which the estimation of position-related parameters, such as TOA and AOA, is performed first, followed by position estimation from those parameters. We have seen that TOA systems are particularly well suited for this purpose and have investigated this technique in more depth. We have also considered implementation issues for UWB ranging systems. ■

REFERENCES

[1] "First report and order 02-48," Federal Communications Commission, Feb. 2002.

[2] Z. Sahinoglu, S. Gezici, and I. Guvenc, *Ultra-Wideband Positioning Systems: Theoretical Limits, Ranging Algorithms, and Protocols*. Cambridge, U.K.: Cambridge Univ. Press, 2008.

[3] *Part 15.4: Wireless Medium Access Control (MAC) and Physical Layer (PHY) Specifications for Low-Rate Wireless Personal Area Networks (LRWPANs)*, IEEE P802.15.4a/D4 (Amendment of IEEE Std. 802.15.4), Jul. 2006.

[4] *High Rate Ultra Wideband PHY and MAC Standard, 1st Ed.*, ECMA-368, Dec. 2005. [Online]. Available: http://www.ecma-international.org/publications/files/ECMA-ST/ECMA-368.pdf

[5] R. Kohno, *Interpretation and future modification of Japanese regulation for UWB*, IEEE P802.15-06/261r0, May 16, 2006.

[6] The Commission of the European Communities, "Commission decision of 21 February 2007 on allowing the use of the radio spectrum for equipment using ultra-wideband technology in a harmonised manner in the community," *Official J. Eur. Union*, Feb. 23, 2007. [Online]. Available: http://eur-lex.europa.eu/LexUriServ/site/en/oj/2007/l_055/l_05520070223en00330036.pdf

[7] M. Z. Win and R. A. Scholtz, "Impulse radio: How it works," *IEEE Commun. Lett.*, vol. 2, no. 2, pp. 36–38, 1998.

[8] P. Runkle, J. McCorkle, T. Miller, and M. Welborn, "DS-CDMA: The modulation technology of choice for UWB communications," in *Proc. IEEE Int. Conf. Ultrawideband Syst. Technol. (UWBST)*, Baltimore, MD, Nov. 16–19, 2003, pp. 364–368.

[9] E. Saberinia and A. H. Tewfik, "Multi-user UWB-OFDM communications," in *Proc. IEEE Pacific Rim Conf. Commun., Comput. Signal Process. (PACRIM)*, Victoria, Canada, Aug. 28–30, 2003, vol. 1, pp. 127–130.

[10] S. Gezici, Z. Tian, G. B. Giannakis, H. Kobayashi, A. F. Molisch, H. V. Poor, and Z. Sahinoglu, "Localization via ultra-wideband radios: A look at positioning aspects for future sensor networks," *IEEE Signal Process. Mag.*, vol. 22, pp. 70–84, Jul. 2005.

[11] K. Siwiak and J. Gabig, *IEEE 802.15.4IGa informal call for application response, contribution #11*, IEEE 802.15-04/266r0, Jul. 2003. [Online]. Available: http://www.ieee802.or/15/pub/TG4a.html

[12] *Local and Metropolitan Area Networks Specific Requirements, Part 15.4: Wireless Medium Access Control (MAC) and Physical Layer (PHY) Specifications for Low-Rate Wireless Personal Area Networks (LR-WPANs)*, 802.15.4, May 2003. [Online]. Available: http://standards.ieee.org/getieee802/download/802.15.4-2003.pdf

[13] "IEEE 802.15 WPAN low rate alternative PHY task group 4a (TG4a)." [Online]. Available: http://www.ieee802.org/15/pub/TG4a.html

[14] I. Oppermann, M. Hamalainen, and J. I., Eds., *UWB Theory and Applications*. New York: Wiley, 2004.

[15] K. Pahlavan and A. H. Levesque, *Wireless Information Networks*, 2nd ed. Hoboken, NJ: Wiley, 2005.

[16] M. Ghavami, L. B. Michael, and R. Kohno, *Ultra Wideband Signals and Systems in Communication Engineering*, 2nd ed. West Sussex, U.K.: Wiley, 2007.

[17] S. Gezici, "A survey on wireless position estimation," *Wireless Pers. Commun.*, vol. 44, no. 3, pp. 263–282, Feb. 2008.

[18] F. Gustafsson and F. Gunnarsson, "Mobile positioning using wireless networks," *IEEE Signal Process. Mag.*, vol. 22, pp. 41–53, Jul. 2005.

[19] A. J. Weiss, "Direct position determination of narrowband radio frequency transmitters," *IEEE Signal Process. Lett.*, vol. 11, pp. 513–516, May 2004.

[20] Y. Qi, H. Kobayashi, and H. Suda, "Analysis of wireless geolocation in a non-line-of-sight environment," *IEEE Trans. Wireless Commun.*, vol. 5, pp. 672–681, Mar. 2006.

[21] Y. Qi, "Wireless geolocation in a non-line-of-sight environment," Ph.D. dissertation, Princeton Univ., Princeton, NJ, Dec. 2004.

[22] A. F. Molisch, K. Balakrishnan, C. C. Chong, S. Emami, A. Fort, J. Karedal, J. Kunisch, H. Schantz, U. Schuster, and K. Siwiak, *IEEE 802.15.4a channel model—Final report*, Sep. 2004. [Online]. Available: http://www.ieee802.org/15/pub/TG4a.html

[23] J. J. Caffery, *Wireless Location in CDMA Cellular Radio Systems*. Boston, MA: Kluwer Academic, 2000.

[24] A. Mallat, J. Louveaux, and L. Vandendorpe, "UWB based positioning in multipath channels: CRBs for AOA and for hybrid TOA-AOA based methods," in *Proc. IEEE Int. Conf. Commun. (ICC)*, Glasgow, Scotland: U.K., Jun. 2007.

[25] J.-Y. Lee and R. A. Scholtz, "Ranging in a dense multipath environment using an UWB radio link," *IEEE J. Sel. Areas Commun.*, vol. 20, pp. 1677–1683, Dec. 2002.

[26] W. C. Lindsey and M. K. Simon, *Phase and Doppler Measurements in Two-Way Phase-Coherent Tracking Systems*. New York: Dover, 1991.

[27] G. L. Turin, "An introduction to matched filters," *IRE Trans. Inf. Theory*, vol. IT-6, pp. 311–329, Jun. 1960.

[28] Y. Qi, H. Kobayashi, and H. Suda, "On time-of-arrival positioning in a multipath environment," *IEEE Trans. Veh. Technol.*, vol. 55, pp. 1516–1526, Sep. 2006.

[29] I. Guvenc and Z. Sahinoglu, "Threshold-based TOA estimation for impulse radio UWB systems," in *Proc. IEEE Int. Conf. UWB (ICU)*, Zurich, Switzerland, Sep. 2005, pp. 420–425.

[30] S. Gezici, Z. Sahinoglu, A. F. Molisch, H. Kobayashi, and H. V. Poor, "Two-step time of arrival estimation for pulse based ultra-wideband systems," *EURASIP J. Advances Signal Process.*, vol. 2008, 2008.

[31] L. Yang and G. B. Giannakis, "Timing ultra-wideband signals with dirty templates," *IEEE Trans. Commun.*, vol. 53, pp. 1952–1963, Nov. 2005.

[32] C. Botteron, A. Host-Madsen, and M. Fattouche, "Cramer–Rao bounds for the estimation of multipath parameters and mobiles' positions in asynchronous DS-CDMA systems," *IEEE Trans. Signal Process.*, vol. 52, pp. 862–875, Apr. 2004.

[33] H. V. Poor, *An Introduction to Signal Detection and Estimation*. New York: Springer-Verlag, 1994.

[34] C. E. Cook and M. Bernfeld, *Radar Signals: An Introduction to Theory and Applications*. New York: Academic, 1970.

[35] F. Ramirez-Mireles and R. A. Scholtz, "Multiple-access performance limits with time hopping and pulse-position modulation," in *Proc. IEEE Military Commun. Conf. (MILCOM)*, Boston, MA, Oct. 1998, pp. 529–533.

[36] J. J. Caffery and G. L. Stuber, "Subscriber location in CDMA cellular networks," *IEEE Trans. Veh. Technol.*, vol. 47, pp. 406–416, May 1998.

[37] L. Cong and W. Zhuang, "Hybrid TOA/AOA mobile user location for wideband CDMA cellular systems," *IEEE Trans. Wireless Commun.*, vol. 1, pp. 439–447, Jul. 2002.

[38] A. Catovic and Z. Sahinoglu, "The Cramer–Rao bounds of hybrid TOA/RSS and TDOA/RSS location estimation schemes," *IEEE Commun. Lett.*, vol. 8, pp. 626–628, Oct. 2004.

[39] R. I. Reza, "Data fusion for improved TOA/TDOA position determination in wireless systems," Ph.D. dissertation, Virginia Tech., Blacksburg, 2000.

[40] C. Nerguizian, C. Despins, and S. Affes, "Framework for indoor geolocation using an intelligent system," in *Proc. 3rd IEEE Workshop Wireless LANs*, Newton, MA, Sep. 2001.

[41] M. Triki, D. T. M. Slock, V. Rigal, and P. Francois, "Mobile terminal positioning via power delay profile fingerprinting: Reproducible validation simulations," in *Proc. IEEE Veh. Technol. Conf. (VTC)*, Montreal, PQ: Canada, Sep. 25–28, 2006.

[42] F. Althaus, F. Troesch, and A. Wittneben, "UWB geo-regioning in rich multipath environment," in *Proc. IEEE Veh. Technol. Conf. (VTC)*, Dallas, TX, Sep. 2005, vol. 2, pp. 1001–1005.

[43] C. Nerguizian, C. Despins, and S. Affes, "Geolocation in mines with an impulse response fingerprinting technique and neural networks," *IEEE Trans. Wireless Commun.*, vol. 5, pp. 603–611, Mar. 2006.

[44] A. H. Sayed, A. Tarighat, and N. Khajehnouri, "Network-based wireless location," *IEEE Signal Process. Mag.*, vol. 22, pp. 24–40, Jul. 2005.

[45] L. Cong and W. Zhuang, "Non-line-of-sight error mitigation in mobile location," *IEEE Trans. Wireless Commun.*, vol. 4, pp. 560–573, Mar. 2005.

[46] R. Casas, A. Marco, J. J. Guerrero, and J. Falco, "Robust estimator for non-line-of-sight error mitigation in indoor localization," *EURASIP J. Appl. Signal Process.*, vol. 2006, 2006.

[47] P. C. Chen, "A non-line-of-sight error mitigation algorithm in location estimation," in *Proc. IEEE Int. Conf. Wireless Commun. Netw. (WCNC)*, New Orleans, LA, Sep. 1999, vol. 1, pp. 316–320.

[48] J. J. Caffery and G. L. Stuber, "Overview of radiolocation in CDMA cellular systems," *IEEE Commun. Mag.*, vol. 36, pp. 38–45, Apr. 1998.

[49] S. Al-Jazzar and J. J. Caffery, "ML and bayesian TOA location estimators for NLOS environments," in *Proc. IEEE Veh. Technol. Conf. (VTC)*, Vancouver, BC, Sep. 2002, vol. 2, pp. 1178–1181.

[50] W. Kim, J. G. Lee, and G. I. Jee, "The interior-point method for an optimal treatment of bias in trilateration location," *IEEE Trans. Veh. Technol.*, vol. 55, pp. 1291–1301, Jul. 2006.

[51] M. McGuire, K. N. Plataniotis, and A. N. Venetsanopoulos, "Location of mobile terminals using time measurements and survey points," *IEEE Trans. Veh. Technol.*, vol. 52, pp. 999–1011, Jul. 2003.

[52] S. Gezici, H. Kobayashi, and H. V. Poor, "A new approach to mobile position tracking," in *Proc. IEEE Sarnoff Symp.*

Adv. Wired Wireless Commun., Ewing, NJ, Mar. 2003, pp. 204–207.

[53] T.-N. Lin and P.-C. Lin, "Performance comparison of indoor positioning techniques based on location fingerprinting in wireless networks," in *Proc. Int. Conf. Wireless Netw., Commun. Mobile Comput.*, Jun. 2005, vol. 2, pp. 1569–1574.

[54] J. Kwon, B. Dundar, and P. Varaiya, "Hybrid algorithm for indoor positioning using wireless LAN," in *Proc. IEEE Veh. Technol. Conf. (VTC)*, Los Angeles, CA, Sep. 2004, vol. 7, pp. 4625–4629.

[55] R. O. Duda, P. E. Hart, and D. G. Stork, *Pattern Classification*, 2nd ed. New York: Wiley-Interscience, 2000.

[56] A. J. Smola and B. Scholkopf, "A tutorial on support vector regression," *Statist. Comput.*, vol. 14, pp. 199–222, 2004.

[57] A. Taok, N. Kandil, S. Affes, and S. Georges, "Fingerprinting localization using ultra-wideband and neural networks," in *Proc. Int. Symp. Signals, Syst. Electron.*, Jul. 30–Aug. 2, 2006, pp. 529–532.

[58] M.-A. Pallas and G. Jourdain, "Active high resolution time delay estimation for large BT signals," *IEEE Trans. Signal Process.*, vol. 39, pp. 781–788, Apr. 1991.

[59] B. Alavi and K. Pahlavan, "Modeling of the TOA-based distance measurement error using UWB indoor radio measurements," *IEEE Commun. Lett.*, vol. 10, pp. 275–277, Apr. 2006.

[60] H. Celebi, I. Guvenc, and H. Arslan, "On the statistics of channel models for UWB ranging," in *Proc. IEEE Sarnoff Symp.*, Princeton, NJ, Mar. 2006.

[61] B. Alavi and K. Pahlavan, "Analysis of undetected direct path in time of arrival based UWB indoor geolocation," in *Proc. IEEE Veh. Technol. Conf. (VTC)*, Sep. 2005, vol. 4, pp. 2627–2631.

[62] B. Alavi and K. Pahlavan, "Bandwidth effect on distance error modeling for indoor geolocation," in *Proc. IEEE Pers., Indoor Mobile Radio Commun. (PIMRC)*, Beijing, China, Sep. 2003, vol. 3, pp. 2198–2202.

[63] Z. Sahinoglu and I. Guvenc, "Multiuser interference mitigation in noncoherent UWB ranging via nonlinear filtering," *EURASIP J. Wireless Commun. Netw.*, vol. 2006, 2006.

[64] K. Pahlavan, P. Krishnamurthy, and J. Beneat, "Wideband radio channel modeling for indoor geolocation applications," *IEEE Commun. Mag.*, vol. 36, pp. 60–65, Apr. 1998.

[65] M. P. Wylie and J. Holtzman, "The non-line of sight problem in mobile location estimation," in *Proc. IEEE Int. Conf. Universal Pers. Commun.*, Cambridge, MA, Sep. 1996, pp. 827–831.

[66] J. Borras, P. Hatrack, and N. B. Mandayam, "Decision theoretic framework for NLOS identification," in *Proc. IEEE Veh. Technol. Conf. (VTC)*, Ontario, Canada, May 1998, vol. 2, pp. 1583–1587.

[67] S. Gezici, H. Kobayashi, and H. V. Poor, "Non-parametric non-line-of-sight identification," in *Proc. IEEE Veh. Technol. Conf. (VTC)*, Orlando, FL, Oct. 2003, vol. 4, pp. 2544–2548.

[68] S. Al-Jazzar, J. J. Caffery, and H-R. You, "A scattering model based approach to NLOS mitigation in TOA location systems," in *Proc. IEEE Veh. Technol. Conf. (VTC)*, Birmingham, AL, May 2002, pp. 861–865.

[69] Y. Shimizu and Y. Sanada, "Accuracy of relative distance measurement with ultra wideband system," in *Proc. IEEE Conf. Ultra Wideband Syst. Technol. (UWBST)*, Reston, VA, Nov. 2003, pp. 374–378.

[70] D. Dardari and M. Z. Win, "Threshold-based time-of-arrival estimators in UWB dense multipath channels," in *Proc. IEEE Int. Conf. Commun. (ICC)*, Istanbul, Turkey, Jun. 2006, vol. 10, pp. 4723–4728.

[71] V. S. Somayazulu, J. R. Foerster, and S. Roy, "Design challenges for very high data rate UWB systems," in *Conf. Rec. 36th Asilomar Conf. Signals, Syst. Comput.*, Nov. 2002, vol. 1, pp. 717–721.

[72] E. A. Homier and R. A. Scholtz, "Rapid acquisition of ultra-wideband signals in the dense multipath channel," in *Proc. IEEE Conf. Ultrawideband Syst. Technol. (UWBST)*, Baltimore, MD, May 2002, pp. 105–109.

[73] I. Guvenc and H. Arslan, "Comparison of two searchback schemes for non-coherent TOA estimation in IR-UWB systems," in *Proc. IEEE Sarnoff Symp.*, Princeton, NJ, Mar. 2006.

[74] I. Guvenc, Z. Sahinoglu, A. F. Molisch, and P. Orlik, "Non-coherent TOA estimation in IR-UWB systems with different signal waveforms," in *Proc. IEEE Int. Workshop Ultrawideband Netw. (UWBNETS)*, Boston, MA, Oct. 2005, pp. 245–251.

[75] I. Guvenc and Z. Sahinoglu, "TOA estimation with different IR-UWB transceiver types," in *Proc. IEEE Int. Conf. UWB (ICU)*, Zurich, Switzerland, Sep. 2005, pp. 426–431.

[76] C. Falsi, D. Dardari, L. Mucchi, and M. Z. Win, "Time of arrival estimation for UWB localizers in realistic environments," *EURASIP J. Appl. Signal Process.*, pp. 1–13, 2006.

[77] S. Gezici, H. Kobayashi, H. V. Poor, and A. F. Molisch, "Performance evaluation of impulse radio UWB systems with pulse-based polarity randomization," *IEEE Trans. Signal Process.*, vol. 53, pp. 2537–2549, Jul. 2005.

[78] S. Gezici, A. F. Molisch, H. V. Poor, and H. Kobayashi, "The trade-off between processing gains of an impulse radio UWB system in the presence of timing jitter," *IEEE Trans. Commun.*, vol. 55, pp. 1504–1515, Aug. 2007.

[79] Y.-P. Nakache and A. F. Molisch, "Spectral shaping of UWB signals for time-hopping impulse radio," *IEEE J. Select. Areas Commun*, vol. 24, pp. 738–744, Apr. 2006.

[80] I. Lakkis, *Pulse compression for TG4a*, Jul. 2005. [Online]. Available: http://www.ieee802.org/15/pub/2005/15-05-0456-00-004a-pulse-compression.ppt

[81] I. Lakkis and S. Safavi, *Band plan, PRF, preamble & modulation for TG4a*, Apr. 2005. [Online]. Available: http://grouper.ieee.org/groups/802/15/pub/2005/15-05-0250-01-004a-revised-frequency-plan-and-prf-proposal-tg4a.ppt

[82] Z. Sahinoglu and S. Gezici, "Ranging for IEEE 802.15.4a ultra-wideband devices," in *Proc. IEEE Wireless Microw. Tech. Conf. (WAMICON 2006)*, Clearwater, FL, Dec. 2006, pp. 1–5.

[83] A. Azakkour, M. Regis, F. Pourchet, and G. Alquie, "A new integrated monocycle generator and transmitter for ultra-wideband communications," in *Proc. IEEE Radio Freq. IC Symp.*, Jun. 2005, pp. 79–82.

[84] S. Iida, K. Tanaka, H. Suzuki, N. Yoshikawa, N. Shoji, B. Griffiths, D. Mellor, F. Hayden, I. Butler, and J. Chatwin, "A 3.1 to 5 GHz CMOS DSSS UWB transceiver for WPANs," in *Proc. IEEE Int. Solid-State Circuits Conf. (ISSCC 2005)*, Feb. 2005, vol. 1, pp. 214–215.

[85] D. D. Wentzloff and A. P. Chandrakasan, "Gaussian pulse generators for subbanded ultra-wideband transmitters," *IEEE Trans. Microwave Theory Tech.*, vol. 54, pp. 1647–1655, Jun. 2006.

[86] H. Kim, Y. Joo, and S. Jung, "A tunable CMOS UWB pulse generator," in *Proc. IEEE Int. Conf. Ultra-Wideband*, Waltham, MA, Sep. 24–27, 2006, pp. 109–112.

[87] H. Kim and D. P. ad Y. Joo, "All-digital low-power CMOS pulse generator for UWB system," *Electron. Lett.*, vol. 40, pp. 1534–1535, Nov. 2004.

[88] Y. Shimizu, Y. Takeuchi, and Y. Sanada, "Novel positioning system with extremely low power radio," in *Proc. IEEE Conf. Ultrawideband Syst. Technol. (UWBST)*, Kyoto, Japan, May 2004, pp. 391–394.

[89] W. Yao and Y. Wang, "Direct antenna modulation & A promise for ultra-wideband (UWB) transmitting," in *Proc. IEEE MTT-S Int. Microw. Symp. Dig.*, Jun. 2004, vol. 2, pp. 1273–1276.

[90] L. Smaini, C. Tinella, D. Helal, C. Stoecklin, L. Chabert, C. Devaucelle, R. Cattenoz, N. Rinaldi, and D. Belot, "Single-chip CMOS pulse generator for uwb systems," *IEEE J. Solid-State Circuits*, vol. 41, pp. 1551–1561, Jul. 2006.

[91] Y. Jeong, S. Jung, and J. Liu, "A CMOS impulse generator for UWB wireless communication systems," in *Proc. Int. Symp. Circuits Syst. (ISCAS 2004)*, May 2004, vol. 4, pp. 129–132.

[92] K. Li, "UWB bandpass filter: Structure, performance and application to UWB pulse generation," in *Proc. Asia-Pacific Microw. Conf. (APMC 2005)*, Dec. 2005, vol. 1.

[93] K. Li, "Experimental study on UWB pulse generation using UWB bandpass filters," in *Proc. IEEE Int. Conf. Ultra-Wideband*, Waltham, MA, Sep. 2006, pp. 103–108.

[94] B. Jung, Y.-H. Tseng, J. Harvey, and R. Harjani, "Pulse generator design for UWB IR communication systems," in *Proc. IEEE Int. Symp. Circuits Syst. (ISCAS 2005)*.

[95] X. Zhang, S. Ghosh, and M. Bayoumi, "A low power cmos uwb pulse generator," in *Proc. 48th Midwest Symp. Circuits Syst.*, Aug. 2005, vol. 2, pp. 1410–1413.

[96] T. Terada, S. Yoshizumi, M. Muqsith, Y. Sanada, and T. Kuroda, "A CMOS ultra-wideband impulse radio transceiver for 1-Mb/s data communications and ±2.5-cm range finding," *IEEE J. Solid-State Circuits*, vol. 41, pp. 891–898, Apr. 2006.

[97] R. Harjani, J. Harvey, and R. Sainati, "Analog/RF physical layer issues for UWB systems," in *Proc. 17th Int. Conf. VLSI Design*, Mumbai, India, Jan. 2004, pp. 941–948.

[98] G. L. Puma, A. Wiesbauer, and C. Sander, "Fully integrated power amplifier in CMOS technology, optimized for UWB transmitters," in *Proc. IEEE Radio Freq. Integr. Circuits (RFIC) Symp.*, Jun. 2004, pp. 87–90.

[99] S. Andersson, C. Svensson, and Drugge, "Wideband LNA for a multistandard wireless receiver in 0.18 μm CMOS," in *Proc. 29th Eur. Solid-State Circuits Conf. (ESSCIRC 2003)*, Sep. 16–18, 2003, pp. 655–658.

[100] H. C. Hsu, Z. W. Wang, and G. K. Ma, "A low power CMOS full-band UWB power amplifier using wideband RLC matching method," in *Proc. IEEE Int. Conf. Electron Devices Solid-State Circuits*, Dec. 2005, pp. 233–236.

[101] C. Lu, A. V. Pham, and M. Shaw, "A CMOS power amplifier for full-band uwb transmitters," in *Proc. IEEE Radio Freq. Integr. Circuits (RFIC) Symp.*, Jun. 11–13, 2006.

[102] J. Powell, "Antenna design for ultra wideband radio," M.S. thesis, Massachusetts Inst. of Technol., May 2004.

[103] Z. N. Chen and M. Y. W. Chia, *Broadband Planar Antennas: Design and Applications*. West Sussex, U.K.: Wiley, 2006.

[104] D. Lamensdorf and L. Susman, "Baseband-pulse-antenna techniques," *IEEE Antennas Propag. Mag.*, pp. 20–30, Feb. 1994.

[105] X. H. Wu, Z. N. Chen, and N. Yang, "Optimization of planar diamond antenna for single/multi-band UWB wireless communications," *Microw. Optical Technol. Lett.*, vol. 42, no. 6, pp. 451–455, 2004.

[106] M. J. Ammann and Z. N. Chen, "A wideband shorted planar monopole with bevel," *IEEE Trans. Antennas Propag.*, vol. 51, pp. 901–903, Nov. 2003.

[107] D. Ghosh, A. De, M. C. Taylor, T. K. Sarkar, M. C. Wicks, and E. L. Mokole, "Transmission and reception by ultra-wideband (UWB) antennas," *IEEE Antennas Propag. Mag.*, vol. 48, pp. 67–99, Oct. 2006.

[108] Z. N. Chen, M. J. Ammann, and M. Y. W. Chia, "Broadband square annular planar monopoles," *Microw. Opt. Technol. Lett.*, vol. 36, no. 6, pp. 449–454, Mar. 2003.

[109] D. Valderas, J. Melendez, and I. Sancho, "Some design criteria for UWB planar monopole antennas: Application to a slotted rectangular monopole," *Microw. Opt. Technol. Lett.*, vol. 46, no. 1, pp. 6–11, Jul. 2005.

[110] M. J. Ammann and Z. N. Chen, "An asymmetrical feed arrangement for improved impedance bandwidth of planar monopole antennas," *Microw. Opt. Technol. Lett.*, vol. 40, no. 2, pp. 156–158, 2004.

[111] E. Antonino-Daviu, M. Cabedo-Fabres, M. Ferrando-Bataller, and A. Valero-Nogueira, "Wideband double-fed planar monopole antennas," *Electron. Lett.*, vol. 39, no. 23, pp. 1635–1636, Nov. 2003.

[112] M. Y. W. C. Z. N. Chen, M. J. Ammann, and T. S. P. See, "Circular annular planar monopoles with EM coupling," *Proc. Inst. Elect. Eng. Microw. Antennas, Propag.*, vol. 150, pp. 269–273, Aug. 2003.

[113] Z. N. Chen, M. J. Ammann, X. Qing, X. H. Wu, T. S. P. See, and A. Cai, "Planar antennas," *IEEE Micro*, vol. 7, pp. 63–73, Dec. 2006.

[114] M. A. Peyrot-Solis, G. M. Galvan-Tejada, and H. Jardon-Aguilar, "State of the art in ultra-wideband antennas," in *Proc. 2nd Int. Conf. Electr. Electron. Eng.*, Sep. 2005, pp. 101–105.

[115] W. Namgoong, "A channelized digital ultra-wideband receiver," *IEEE Trans. Wireless Commun.*, vol. 2, pp. 502–510, May 2003.

[116] P. P. Newaskar, R. Blazquez, and A. P. Chandrakasan, "A/D precision requirements for an ultra-wideband radio receiver," in *Proc. IEEE Workshop Signal Process. Syst. (SIPS 2002)*, Oct. 16–18, 2002, pp. 270–275.

[117] R. Blazquez, F. S. Lee, D. D. Wentzloff, P. P. Newaskar, J. D. Powell, and A. P. Chandrakasan, "Digital architecture for an ultra-wideband radio receiver," in *Proc. IEEE 58th Veh. Technol. Conf. (VTC 2003-Fall)*, Orlando, FL, Oct. 6–9, 2003, vol. 2, pp. 1303–1307.

[118] M. Verhelst, W. Vereecken, M. Steyaert, and W. Dehaene, "Architectures for low power ultra-wideband radio receivers in the 3.1-5 GHz band for data rates < 10 Mbps," in *Proc. IEEE Int. Symp. Low Power Electron. Design (ISLPED 2004)*, Aug. 11–19, 2004, pp. 280–285.

[119] A. F. Molisch, Y. P. Nakache, P. Orlik, J. Zhang, Y. Wu, S. Gezici, S. Y. Kung, H. Kobayashi, H. V. Poor, Y. G. Li, H. Sheng, and A. Haimovich, "An efficient low-cost time-hopping impulse radio for high data rate transmission," *EURASIP J. Appl. Signal Process. (Special Issue on UWB and State of the Art)*, vol. 2005, no. 3, pp. 397–412, Mar. 2005.

[120] H. Xie, S. Fan, X. Wang, A. Wang, Z. Wang, H. Chen, and B. Zhao, "A pulse-based non-carrier 7.5 GHz UWB transceiver SoC with on-chip ADC," in *Proc. 8th Int. Conf. Solid-State Integr. Circuit Technol. (ICSICT 2006)*, Shanghai, China, Oct. 23–26, 2006, pp. 1804–1807.

[121] I. S.-C. Lu, N. Weste, and S. Parameswaran, "ADC precision requirement for digital ultra-wideband receivers with sublinear front-ends: A power and performance perspective," in *Proc. 19th Int. Conf. VLSI Design (VLSID 2006)*, Jan. 3–7, 2006.

[122] R. Thirugnanam, D. S. Ha, and S. S. Choi, "Design of a 4-bit 1.4 Gsamples/s low power folding ADC for DS-CDMA UWB transceivers," in *Proc. IEEE Int. Conf. Ultra-Wideband (ICU 2005)*, Zurich, Switzerland, Sep. 5–8, 2005, pp. 536–541.

[123] S. Hoyos, B. M. Sadler, and G. R. Arce, "Monobit digital receivers for ultrawideband communications," *IEEE Trans. Wireless Commun.*, vol. 4, pp. 1337–1344, Jul. 2005.

[124] R. Blazquez, P. P. Newaskar, F. S. Lee, and A. P. Chandrakasan, "A baseband processor for pulsed ultra-wideband signals," in *Proc. IEEE Custom Integr. Circuits Conf.*, Oct. 3–6, 2004, pp. 587–590.

[125] S. Hoyos and B. M. Sadler, "Ultra-wideband analog-to-digital conversion via signal expansion," *IEEE Trans. Veh. Technol.*, vol. 54, pp. 1609–1622, Sep. 2005.

[126] H. Lee, D. Ha, and H. Lee, "Toward digital UWB radios: Part I—Frequency domain UWB receiver with 1 bit ADCs," in *Proc. IEEE Conf. Ultrawideband Syst. Technol. (UWBST)*, Kyoto, Japan, May 2004, pp. 248–252.

[127] M. S.-W. Chen and R. W. Brodersen, "A subsampling uwb radio architecture by analytic signaling," in *Proc. IEEE Int. Conf. Acoust., Speech, Signal Process. (ICASSP)*, Montreal, PQ, Canada.

[128] Y. Vanderperren, W. Dehaene, and G. Leus, "A flexible low power subsampling UWB receiver based on line spectrum estimation methods," in *Proc. Int. Conf. Commun. (ICC 2006)*, Istanbul, Turkey, Jun. 2006, vol. 10, pp. 4694–4699.

ABOUT THE AUTHORS

Sinan Gezici (Member, IEEE) received the B.S. degree from Bilkent University, Turkey, in 2001 and the Ph.D. degree in electrical engineering from Princeton University, Princeton, NJ, in 2006.

From April 2006 to January 2007, he was a Visiting Member of Technical Staff with Mitsubishi Electric Research Laboratories, Cambridge, MA. Since February 2007, he has been an Assistant Professor in the Department of Electrical and Electronics Engineering, Bilkent University. His research interests are in the areas of signal detection, estimation and optimization theory, and their applications to wireless communications and localization systems. Among his publications in these areas is the recent book *Ultra-Wideband Positioning Systems: Theoretical Limits, Ranging Algorithms, and Protocols* (Cambridge, U.K.: Cambridge University Press, 2008).

H. Vincent Poor (Fellow, IEEE) received the Ph.D. degree in electrical engineering and computer science from Princeton University, Princeton, NJ, in 1977.

From 1977 until 1990, he was on the faculty of the University of Illinois at Urbana-Champaign. Since 1990, he has been on the faculty of Princeton, where he is the Michael Henry Strater University Professor of Electrical Engineering and Dean of the School of Engineering and Applied Science. His research interests are in the areas of stochastic analysis, statistical signal processing, and their applications in wireless networks and related fields. Among his publications in these areas are the recent books *MIMO Wireless Communications* (Cambridge, U.K.: Cambridge University Press, 2007) and *Quickest Detection* (Cambridge, U.K.: Cambridge University Press, 2009).

Dr. Poor is a member of the National Academy of Engineering, a Fellow of the American Academy of Arts and Sciences, and a former Guggenheim Fellow. He is also a Fellow of the Institute of Mathematical Statistics, the Optical Society of America, and other organizations. In 1990, he was President of the IEEE Information Theory Society, and in 2004–2007 he was Editor-in-Chief of the IEEE TRANSACTIONS ON INFORMATION THEORY. He received the 2005 IEEE Education Medal. Recent recognition of his work includes the 2007 IEEE Marconi Prize Paper Award from the IEEE Communications Society, the 2007 Technical Achievement Award from the IEEE Signal Processing Society, and the 2008 Aaron D. Wyner Award from the IEEE Information Theory Society.